# THE EFFECT OF MICROSTRUCTURE ON THE THERMAL FATIGUE RESISTANCE OF INVESTMENT CAST AND WROUGHT AISI H13 HOT WORK DIE STEEL:

P.W. Hochanadel and G.R. Edwards, Colorado School of Mines, Golden, CO, 80401; M.C. Maguire and M.D. Baldwin, Sandia National Laboratories, Albuquerque, NM, 87185.

## Abstract

Variable thickness plate investment castings of AISI H13 hot work die steel were poured and characterized in the as-cast and heat treated conditions. The characterization included light microscopy and mechanical testing. Wrought samples of standard and premium grade H13 steel were heat treated and characterized similarly for comparison. Microstructural differences were observed in as-cast samples poured to different section thicknesses. Dendrite cell size and carbide morphology constituted the most prominent microstructural differences observed. After a full heat treatment, however, microstructural differences between the wrought material and cast materials were slight regardless of section thickness. The mechanical properties of the cast and heat treated material proved similar to the properties of the standard heat treated wrought material. A thermal fatigue testing unit was designed and built to correlate the heat checking susceptibility of AISI H13 steel to its processing and consequent microstructural condition. Surface hardness decreased significantly with thermal cycling, and heat checking was noticed in as few as 50 cycles. Thermal softening and thermal fatigue susceptibility were quantified and discussed relative to the microstructural conditions created by processing and heat treatment. It was found that the premium grade wrought H13 steel provided the best overall resistance to heat checking; however, the heat-treated cast and as-cast H13 tool steel (made from standard grade wrought H13 tool steel) provided comparable resistance to heat checking in terms of area fraction of heat checking and maximum crack length.

Key Words: Cast Die Steel, Thermal Fatigue, Heat Treatments

1

MASTER

# DISCLAIMER

# DISCLAIMER

**Portions of this document may be illegible in electronic image products. Images are produced from the best available original document.**

## Introduction

The concept of using cast tool steels is not new. An industrial interest in utilizing cast dies has existed both in the United States and in the former Czechoslovakia since the 1950's. This topic has been explored in Japan since the early 1960's. However, the interest in utilizing cast H13 steel declined in the late 1960's and early 1970's due to leadtimes (and thus costs) involved in developing the prototypes. Throughout the 1970's and 1980's, Russian and other European scientists extensively studied cast 5% chromium die steels and various other tool steels. Much of this work involved actual production tests, and little pertinent correlation between the microstructure and properties was discussed. Recently, Chinese investigators have shown interest in cast H13 steel.

Cast die steels were attractive to the die manufacturer and user because of the overall cost-effectiveness of using cast dies or inserts. Figure 1 shows a schematic representation of the various costs in the manufacture of a die casting die. The cost effectiveness may be improved with cast die steels two ways: (1) shaping operations may be minimized, and (2) processing prior to or following the shaping of the material may be simplified. It can be seen from Figure 1 that shaping operation (i.e. die building) costs are typically much greater than thermal processing costs. If the cast die or insert provides an adequate number of runs comparable to the wrought counterpart, then the overall cost is reduced even more.

In the United States, technology transfer has become very important for industry-government cooperative research efforts. At Sandia National Laboratories, a rapid prototyping program named FASTCAST is an example of technology transfer. This program establishes rapid turnaround of precision investment castings via computer programming and computer machine control. Consequently, cast dies and inserts are now being re-considered. The computer-controlled pattern is quickly fabricated by selective laser sintering and stereolithography, effectively minimizing both cost and time.

Besides cost, another problem related to cast dies may be casting microsegregation, an inherent factor in all castings (and to some extent, in many wrought products). This phenomenon, coupled with porosity, produces deleterious properties in castings, and although cast tools may be less-costly, their life may be shorter, thereby

2

decreasing the cost-effectiveness. A number of papers have reported comparable and possibly longer die life for cast dies or components in which the castings were sound[1-6].

The life-limiting property of these materials (such as AISI H13) is "heat checking", in which network cracks are formed from stresses resulting from the constraint of the subsurface material on heating and cooling (i.e. thermal fatigue). Some investigations have claimed that a cast structure aided in the delay of heat checking, and that the cracks did not penetrate as deeply as those in the wrought dies[5]. As a result, the re-tooling of cast dies or inserts was less costly than re-tooling wrought counterparts. These results, were neither correlated with the soundness of the casting nor the actual microstructure. More shallow heat checks in cast molds or inserts allow more re-tooling operations to be performed prior to a mold losing its dimensional accuracy.

A simple thermal cycling device can determine whether these improvements in cast versus wrought dies may be obtained. Industrial tests have shown that wear in cast materials is less than wear in wrought materials. According to Torrey[2,4], the wrought material, because of the smaller grain size, possesses more grain boundary energy. At higher temperatures, oxidation or corrosion occurs more frequently at high energy regions, such as grain boundaries, rather than within each grain. A coarser-grained cast die would consequently not damage as badly as a wrought die. In addition, once a decomposition process such as oxidation occurs, the decomposed area becomes a preferential site for crack initiation and propagation. The observation that heat checking cracks begin at oxidation or corrosion pits has been documented by Wallace[7]. Rostocker[6] thermally cycled tapered disc samples made from both cast and wrought H11 tool steel and found that the cast material resisted heat checking better than its wrought counterpart.

A plethora of information pertaining to the processing, microstructure and mechanical properties of wrought H13 steel and various other hot-work tool steels is available. In addition, numerous publications exist which address the attractiveness of cast dies in terms of cost and die life. However, technical information regarding the cast hot-work tool steels is lacking, and very little information exists correlating the microstructure (as-cast cast and heat treated) with resulting properties. The purpose of

this investigation was to determine the effect of microstructure on heat checking of both wrought and cast H13 tool steel. This study compared the processing of cast and wrought AISI H13 tool steel in terms of microstructure and properties, and, more specifically, determined the influence of the microstructure (i.e. resulting from processing) on the heat checking susceptibility.

## Experimental Procedure

Charge material for the investment cast material was obtained in the form of standard grade wrought AISI H13 steel from Eagle Alloys, Inc. (Jefferson City, Tenn). The composition of the standard grade wrought and cast material is found in Table 1. Plate investment castings were designed to vary the cooling rate during casting, and an example of a wax pattern of the 0.5-in-thick plate casting appears in Figure 2. The castings were melted and poured under 150 torr of argon after vacuum evacuation to 10 millitorr to improve the cleanliness of the material. Both standard grade and premium grade H13 steel were tested for comparison. The premium grade wrought material was obtained from Finkl and Sons, Inc. (Chicago, Ill), and the composition of the premium grade wrought H13 tool steel is found in Table 2. The premium grade wrought H13 tool steel was processed with vacuum arc degassing and vacuum arc remelting. The forging reduction ratio was 12:1. A thermal fatigue testing unit was designed, based on the Uddholms tester[8], and built to test small-scale test samples, since an interest in casting die inserts was the goal of the initial research. Figure 3 illustrates the schematic design of the thermal fatigue testing unit. This apparatus utilized a high-frequency generator as the heating source, and water jets for the cooling source. The entire operation of the machine was computer-controlled. Equipment of this type utilizes the skin effect to heat the outside, while the non-heated core material acts as a constraint to surface expansion and compression, thus developing alternating surface compressive and tensile stresses on heating and cooling, respectively. A calibration curve for the testing apparatus, which shows peak surface and peak center temperature versus generator time on, appears in Figure 4. The samples were approximately 2 inches (55 millimeters) long with a 0.4-in. (10-mm) diameter. In addition, the samples were ground to provide a 0.2-in. (5-mm) flat

4

so that proper evaluation of the surface could be made. Edges of the flat were rounded to prevent stress concentrations. The flat was final-polished to prevent any stress concentration on the surface caused by grinding.

Prior to testing, many samples were rough-machined to a 0.4-in. (10-mm) diameter and heat treated. The cast material was either homogenized, austenitized, and double-tempered, or simply austenitized and double-tempered. The matrix for this investigation is shown in Table 3. The samples were homogenized in an argon atmosphere at 2285°F (1250°C) for four hours, austenitized in a high-temperature molten salt pot at 1835-1865°F (1000-1020°C) for 30 minutes, then cooled by forced-air to room temperature. A rapid cool avoided excessive grain boundary carbide precipitation, which has been shown to be detrimental to the mechanical properties of H13 tool steel[9-13]. Samples were tempered in two stages: (1) at 1095°F (590°C) and (2) at 1110°F (600°C), both of which were in high-temperature molten salts. In each step samples were tempered for two hours and air cooled. The wrought samples, which had been previously annealed for ease of machinability, were austenitized and tempered by a process similar to that of the cast samples.

All samples were subjected to one thousand temperature cycles. The temperature was cycled from room temperature to 1295°F (700°C) and back to room temperature in 7 seconds. Initial hardness and microhardness readings were taken, and then microhardness readings were taken after 50, 150, 350, 550, 750 and 1000 cycles with a LECO M-400A tester using a 200-g load. A LECO R-600 hardness tester was used to determine initial (prior to thermal cycling) Rockwell C hardnesses. In addition, the surface cracking was photographed at various stages of testing. A Leco 2001 Image Analyzer was utilized to count and measure heat checks in the selected standard area on the sample. Lines were marked with a felt pen at 0.5-in. (13-mm) and 0.8-in. (20-mm) positions from the bottom of the sample. Initial and final microstructures were analyzed through light microscopy. Samples were prepared for light microscopy by standard metallographic procedures. Samples were etched with a 2-pct nital etch to reveal the microstructure.

5

## Processing Evaluation

The effects of processing on the microstructure and hardness was evaluated at two levels: (1) primary (casting) and (2) secondary (heat treating). As the plate thickness was increased, the microstructural coarseness, as given by dendrite cell size, increased, which caused corresponding decreases in hardness. The relationship between hardness and dendrite cell size is shown in Figure 5. A linear relationship between hardness and cell size, similar to the results of Spear and Gardner[14], was observed. Photomicrographs of the as-cast 0.5-in. and 1.5-in. plate castings appear in Figure 6. It is evident from Figure 6 that even a difference of one inch in the plate thickness caused significant variation in cast structure. However, the 1.5-in. cast material was found to contain notable amounts of second phase particles (primary carbides and inclusions), primarily in the intercellular regions. Standard inclusion ratings for the 0.5-in. cast material and the as-cast 1.5-in H13 steel were comparable, but the 0.5-in cast material contained fewer interdendritic primary carbides. The ASTM E-45 J-K inclusion rating for these materials is presented in Table 4. As shown in Figure 6, microstructural features could be observed within the interior of the dendritic cells, most probably a subgrain structure formed upon cooling after solidification. After casting, selected samples were subjected to either a partial heat treatment (in which samples are cast, hardened and double-tempered) or a full heat treatment (in which samples are homogenized and then processed according to the partial heat treatment as shown in Table 3). When cast samples were subjected to the partial heat treatment, evidence of the cast structure remained throughout processing as shown in Figure 7. After a full heat treatment, however, evidence for the cast structure was no longer apparent, and this may be seen in Figure 8. The inclusion rating for these materials also appears in Table 4. The heat-treated standard wrought microstructure, which appears in Figure 9, was quite different from any of the other microstructures shown previously, in that the wrought material contained much finer grains, and hence a much finer tempered microstructure. Also, the standard wrought material contained significant fractions amount of both sulfide-type and globular oxide-type inclusions (Table 4). Inclusion ratings for this material this material were quite different from ratings for the premium grade wrought material (a rating of zero for the sulfide-type inclusions, and

6

a rating of 0.5-thin for the globular oxide-type inclusions). In addition, the microstructure for premium grade H13 steel, seen in Figure 10, was slightly different in appearance when compared to the standard H13 alloy. With the exception of the as-cast material, the as-heat treated hardness values were 45 to 47 Rockwell C. The as-cast hardness values for the 0.5-in. plate and the 1.5-in. plate were 55 and 50 Rockwell C, respectively.

The ASTM grain size of the wrought material (in the as-hardened condition) was found to be 9.5 for the standard wrought and 9 for the premium wrought material. It was difficult, however, to determine the grain sizes for the as-cast and the partially heat-treated cast materials, since the grain sizes of these castings were quite coarse, and sub-grains occurred within the dendrite cells. The dendrite cell sizes of as-cast and cast-plus-partially heat-treated H13 steel probably influence properties more than the grain sizes. The ASTM grain size of the fully heat-treated 0.5-in. plate material was found to be 4, while the ASTM grain size of the fully heat-treated 1.5-in. plate material was found to be 2.

### Thermal Fatigue Testing

The samples for this investigation were subjected to 1000 thermal cycles. A time-temperature profile of the thermal cycles is found in Figure 11. The results of these tests included area fraction of heat checks, maximum crack length, and 200-g load surface microhardness values, all recorded as a function of the number of thermal cycles. The area fraction of heat checks observed on the surface of the samples was found to be the best indicator of heat checking severity. The area fraction value displayed the severity of heat checking in three ways: (1) the number of cracks, (2) the crack lengths, and (3) the crack widths (an indication of crack depth). For instance, a sample with many small, shallow cracks would probably have a lower area fraction of heat checks than a sample which contained fewer large, deep cracks. Also, photographs of the surface were taken at 150, 550 and 1000 cycles, and light microscopy was used to observe any microscopic differences in sectioned samples after testing.

Figure 12 shows the variation of hardness with the number of cycles for all

conditions. As expected, the surface microhardness decreased significantly during thermal cycling, since the peak temperature in the thermal cycle (1295°F) was roughly 185°F (100°C) higher than the tempering temperature. From all of the heat-treated samples, it was observed that the surface microhardness values decreased from about 440 VHN to about 290 VHN. Figures 13 and 14 show the variation of the area fraction of heat checks and maximum crack length versus the number of cycles, respectively. All conditions are shown for comparison. The area fraction of heat checks increased monotonically with an increase in the number of thermal cycles. Figure 15 shows the area fraction of heat checks versus the number of thermal cycles for the as-cast 1.5-in. plate material, and error bars at the 95% confidence interval were added to determine the statistical significance of the data. The error bars indicate that the functional relationship between the area fraction of heat checks and the number of cycles cannot be expressly determined from these data, and that further experimentation is needed to clarify any regions of slow crack growth. The maximum crack length varied linearly with the number of thermal cycles. Figure 16 is a summary plot depicting the dependence of area fraction of heat checks and maximum crack length on the sample condition after 1000 thermal cycles. With respect to the area fraction of heat checks (cracking severity), the premium wrought material displayed the best resistance to heat checking, while the as-cast 1.5-in. plate material and fully heat-treated 1.5-in. plate material exhibited good resistance to heat checking. The other materials all exhibited similar resistance to heat checking. Both the premium and standard grade wrought material exhibited the best resistance to crack growth, and the as-cast 0.5-in. plate material exhibited by far the worst resistance to crack growth.

Differences in surface cracking were observed at all stages of testing. Both standard and premium wrought H13 tool steel revealed a similar heat checking configuration. However, the severity of heat checking was noticeably lower for the premium wrought H13 tool steel. Figure 17, which shows the surface of the standard and premium grades of wrought H13 tool steel, reveals how most cracking occurred perpendicular to the maximum hoop stress encountered in the test. In the cast samples (regardless of as-cast or heat-treated cast), a heat checking pattern which was less

8

random than the wrought sample heat checking configuration was observed. Figure 18 shows the surface of the as-cast 1.5-in. plate cast H13 steel samples at various stages in testing. Note that an extra photograph was taken at 50 cycles which indicates that oxidation pits play a role in crack nucleation. The heat checking pattern observed in the cast samples may be less random, since some obvious casting flaws, such as microvoids and microsegregation, were found to provide preferential sites for crack nucleation.

The microstructure of the thermal fatigue samples, with the exception of the as-cast samples, remained essentially the same when observed with light microscopy. Figure 19 shows the microstructures of the 0.5-in. and 1.5-in. plate cast thermal fatigue samples after thermal cycling. Thermal fatigue cracking was found to initiate at and propagate through various inhomogeneities such as inclusions, bulky carbides, grain boundaries, and intercellular regions of compositional variations. Grain boundary attack was the most commonly observed mechanism for thermal fatigue cracking in both wrought and fully heat-treated cast samples. However, cracks were also found to propagate through the grains as well. Figure 20 shows evidence for intergranular cracking in the premium grade wrought sample and the as-cast 1.5-in plate cast H13 steel after 1000 cycles. Grain boundary cracking was also observed in cast and heat-treated cast samples. In the as-cast and partially heat-treated cast samples, thermal fatigue cracking was mainly observed along intercellular (interdendritic) regions. An indication of the intercellular cracking appears in Figure 21, which shows a cross-section of the as-cast 0.5-in. plate cast H13 steel after 1000 cycles.

## Discussion

The expected correlation between hardness and dendrite cell size was found. This dependence has been described by Spear and Gardner[14]. As the dendrite cell size increased, the amount of intercellular primary carbide was found to increase. The inclusion ratings were found to be approximately the same, regardless of casting thickness.

A partial heat treatment, which included austenitization and tempering, did little

to dissolve primary carbides and microsegregation. The homogenization treatment, however, was effective in dissolving the primary alloy carbides, and a previous investigation showed that samples made from low-sulfur cast material which was homogenized prior to hardening and tempering yielded Charpy V-notch impact energies comparable to the values found for premium grade wrought material[15]. The same study showed that the as-cast material had slightly lower impact energies than both the cast and heat-treated and wrought H13 steel. The lower impact energies obtained for the as-cast material were probably the result of more undissolved primary carbides throughout the matrix of the as-cast material. Primary carbides, if not dissolved, have been found to be detrimental to the impact properties and toughness of H13 tool steel[9-13].

Thermal fatigue testing on various conditions of standard H13 tool steel (both cast and wrought) and premium wrought H13 tool steel showed that the premium wrought material was the most resistant to thermal fatigue cracking. In comparing the standard and premium grade wrought materials, the largest difference was found to be in the inclusion ratings. The grains of the premium grade material were found to be slightly larger than the grains of standard grade material (ASTM grain size of 9, compared to 9.5 for the standard wrought material); however, it was highly unlikely that the slightly larger grains caused the improved resistance to heat checking found in premium grade wrought H13 steel. Little difference in thermal fatigue resistance was found to occur in the standard grade wrought, as-cast, partially heat-treated cast or fully heat-treated cast H13 tool steels. However, the differences, as slight as they were, showed that the as-cast and cast and heat treated material performed better than the wrought material with respect to the area fraction of heat checks (or crack severity).

Both the heat check severity (area fraction) and the maximum crack length was found to increase monotonically with the number of thermal cycles. A step-wise relationship between crack growth quantity and thermal cycles has been observedn in a number of investigations[8,16-24]. Woodford and Mowbray, in their investigation of cast nickel-base alloys, discovered two distinct regions; a fast crack growth region and a slow crack growth region[16]. The fast- and slow-growth regions were often observed at several different testing periods until the sample reached its maximum value of thermal fatigue

crack growth. Woodford and Mowbray[16] utilized thin-disc samples containing pre-machined notches. No apparent crack nucleation period was noticed, since the preferential site for crack nucleation was introduced as the notch. The cracks in their investigation began within a fast growth regime, and progressed to a slow crack growth regime. The slow crack regions were explained by deviations in the direction of crack propagation (i.e., when cracks were propagating through regions not favorably positioned to yield rapid cracking). Relatively rapid crack growth was observed during the early stages of testing for most samples in this study. During rapid crack growth, the cracks were observed to merge, thus yielding some of the longer maximum crack lengths observed. The lack of an incubation period for cracking may have resulted from the presence of sufficient surface defects, which allowed cracks to develop more rapidly, as witnessed by Woodford and Mowbray[16]. Rostocker[6] investigated the thermal fatigue behavior of both AISI 4130 steel and AISI H13 tool steel using thin discs containing no pre-machined notches in a fluidized bed. These data and most other heat checking data[6-8,20-24] have been shown to have a crack nucleation region and a rapid thermal fatigue crack growth region, but no slow-growth region. The fact that crack growth (in terms of average and maximum crack lengths) does not always exhibit a slow-growth region often indicates that thermal fatigue cracks have merged, yielding an anomolously high crack length as testing continued. Danzer, et al.[17] normalized their crack length data by dividing the sum of the crack lengths ($\Sigma\; l_i$) at a number of cycles, N by the sum of the crack lengths ($\Sigma\; l_{iF}$) at a designated final number of cycles, $N_F$. The number of cycles was normalized by dividing the number of cycles, N, by a designated final number of cycles, $N_F$. A sigmoidal curve displaying all of the characteristics of incubation, rapid growth and slow growth resulted. As Woodford and Mowbray[16] have discovered, thermal fatigue crack growth may fluctuate between rapid growth and slow growth until the test is terminated. Thermal fatigue cracks observed in this investigation do not clearly manifest well-defined incubation, rapid growth and slow growth regimes. Further testing must be completed to characterize the thermal fatigue cracking of H13 tool steel.

The concern over whether fine grain structure adversely affected the impact properties of either cast or wrought H13 steel was addressed in a previous

11

investigation[15]. A fully heat-treated cast 1.5-in. plate material was discovered to perform as well as its wrought counterpart, while the as-cast material was found to have somewhat lower impact energies. Therefore, when the as-cast or cast, homogenized, hardened and tempered material was used, thermal fatigue properties were observed to be slightly better (although not statistically significant) than those of the wrought counterpart. In fact, the fully heat-treated cast 1.5-in. plate material performed slightly better than its wrought counterpart in both thermal fatigue resistance and in impact energy absorbed. Woodford and Mowbray[16] also found, in general, that coarser-grained material performed better (in terms of crack growth rate), than fine-grained material.

Appearance of the heat checking depended upon whether the material was wrought or cast, a fact attributed to the surface defects in the cast material. Several crack nucleation sites were identified in this investigation. The nucleation sites included oxidation pits, grain boundaries, oxide or sulfide inclusions, intercellular regions, primary carbides, and microvoids. These surface flaws act as stress raisers which allow sufficient plastic deformation to occur during thermal cycling. Danzer, et al.[17], also observed that inclusions and bulky carbides or carbide stringers acted as nucleation sites for thermal fatigue cracking. Several cracks were oxide-filled, and grain boundary attack by oxidation is well documented in thermal fatigue testing[16,19,25,26]. This observation does not necessarily mean that grain boundary oxidation is the controlling mechanism for heat checking. However, the oxidation of surface defects likely influences the severity of heat checking[27]. Alternating surface compressive and tensile strains on heating and cooling, respectively, probably act in combination with oxidation of the surface and with already existing cracks to nucleate and propagate heat checks. The dependence of oxidation on the thermal fatigue crack growth has been modelled by Rémy et al.[26]. This

why the page Break?

12

dependence was shown to be a function of both oxidation of the matrix and carbides as:

$$(da/dN)_{OX} = (1 - f_c)\alpha_M(1 + K_M(\Delta\epsilon_\epsilon)\Delta t^{1/2} + f_c\alpha_C g(\Delta\epsilon_\epsilon)\Delta t^{1/4} \qquad (1)$$

where a - crack length

  N - Number of cycles

  $f_c$ - effective volume fraction of carbides along the crack path

  $\alpha_M$, $\alpha_C$ - oxidation constants of matrix and carbides under zero stress

  $g(\Delta\epsilon_{IN})$ - function of strain = $\Delta\epsilon_{IN}/\Delta\epsilon_0$ when $\Delta\epsilon_{IN} > \Delta\epsilon_0$; = 1 when $\Delta\epsilon_{IN} \le \Delta\epsilon_0$

  $K_M$, $\Delta\epsilon_0$, - constants

The fracture of the oxides was assumed to take place at each tensile stroke (on cooling for the thermal fatigue test. This model was tested in terms of both isothermal low-cycle fatigue and thermal fatigue of a cast cobalt-based superalloy. This particular model was found to correlate quite well for the thermal fatigue data acquired in their investigation. However, due to the difficulty in obtaining values such as the amount of plastic strain on each cycle and the various constants, no further efforts to fit our data to this model were made.

Another crack nucleation site during thermal cycling was found to be an oxide layer crack. During thermal cycling, an oxide layer was found to build up on the surface of the sample. Since the oxide layer may be considered an elastic material, the oxide will tend to crack on quenching, thus providing a stress concentration (the oxide crack tip) where plastic strain may be increased on subsequent cycles. This in turn will cause a crack to form, and propagation may be random until the crack meets with another high energy region, such as one listed above.

## Summary of Conclusions

1.  The thermal fatigue resistances of various heat treatments of standard grade H13 tool steel were found to be similar. The as-cast and cast and heat treated material performed slightly better than the standard grade wrought material with respect to the heat checking severity (area fraction of heat checking), and the premium grade wrought steel resisted heat checking better than any of the standard grade H13 tool steels tested. Overall, the best condition of standard grade H13 tool steel was determined to be the cast and fully heat-treated 1.5-in. H13 plate.

2.  The best heat checking resistance for H13 tool steel corresponded to the cleanest material. That is, as inclusion content decreased, the thermal fatigue resistance was found to increase. The inclusion content was much lower in the premium grade wrought H13 steel than in the standard grade wrought H13 steel. Since the grain sizes were comparable, the difference in heat checking resistance was attributed to the inclusion content.

3.  The area fraction of heat checking and maximum crack length was found to increase monotonically with the number of cycles. The data lacked the stastical significance to determine whether heat checking followed incubation, rapid crack growth and slow crack growth regimes.

4.  Heat checks were found to nucleate at surface flaws (oxidation pits at inclusions, carbides, grain boundaries, interdendritic regions) and propagate through grain boundaries, sub-grain boundaries, and interdendritic regions.

5.  In the later stages of heat checking, cracks were found to merge, thus obscuring the results of maximum crack length versus number of cycles.

# References

1. Torry, A. and Jones, R.N., "Cast Die Inserts", Metal Treatment and Drop Forging, Nov. 1962, vol. 29, n. 204, pp 1-60.

2. Torry, A., "Cast Dies and Inserts for Drop Forging Work", Iron and Steel, May 1965, vol. 38, n. 5, pp. 211-7, 221.

3. Jones, R.N., "Cast Dies and Die Inserts for Drop Forging" Metal Treatment, Jan. 1966, vol. 33, n. 204, pp. 25-35.

4. Torrey, A., "Wear in Cast Dies", Light Metals and Metal Industry, May 1965, vol. 28, n. 324, pp. 68-9.

5. Wick, C.H., "Forging Dies: Precision Casting Pays Off" Machinery, Oct. 1965, vol. 72, n. 2, pp. 108-11.

6. Rostocker, W., "Thermal Fatigue Resistance of Martensitic Steels", Journal of Materials, 1969, vol. 4, n. 1, pp. 117-44.

7. Wallace, J.W., "Effect of Selected Processing on Compositional Factors on the Failure of H13 as Dies for Aluminum Die Casting", ADCI Die Tech '84 Technical Seminar, Chicago, IL, 1984, pp. 6-37.

8. Malm, S., Svensson, M. and Tidlund, J., "Heat Checking in Hot Work Steels", Bull. Cercle Etud. Met., 1979, vol. 14, n. 5, pp. 339-75.

9. Dorsch, C. and Ried, P.P., "Evaluating the Heat Treatment of Premium Quality H-13 Die Casting Components" NADCA Transactions, 1991, pp. 215-222.

10. Schmidt, M.L., "What Really Influences the Mechanical Properties of H-13 Tool Steel?" NADCA Transactions, 1989, pp. 1-11.

11. Wallace, J.F., Roberts, W., and Hakulinen, E., "Influence of the Cooling Rate on the Microstructure and Toughness of Premium Grade H-13 Die Steels" NADCA Transactions, 1989, pp. 1-4.

12. Berger, C.M., "Effects of Percentage Primary Carbide on the Charpy V-Notch Impact Strength of Premium H-13 Die Steel", NADCA Transactions, 1989, pp. 1-4.

13. Roberts, W. and Norström, L.-Å.,"Premium Die Steel and Heat Treatment Solutions for the 1990's", NADCA Transactions, 1987, pp. 1-12.

14.     Spear, R.E. and Gardner, G.R., "Dendrite Cell Size", <u>Trans. Amer. Foundry Soc.</u>, 1963, vol. 71, pp. 209-215.

15.     Hochanadel, P.W. and Edwards, G.R., "Effects of Microstructure on the Thermal Fatigue Resistance of Investment Cast and Wrought AISI H13 Steel", Internal report to the Colorado School of Mines, March, 1995.

16.     Woodford, D.A., and Mowbray, D.F, "Effect of Material Characteristics and Test Variables on Thermal Fatigue of Cast Superalloys. A Review", <u>Mat. Sci. and Eng.</u>, 1974, vol .16, pp.5-43.

17.     Danzer, R., Sturm, F., Schindler, A. and Zleppnig, W.,"Thermal Fatigue Cracks in Pressure Die Casting Dies", <u>Gießerei-Praxis</u>, October 1983, No. 19/20, pp. 288-297.

18.     Artinger, I. and Becker, L., " Thermal Fatigue Test for Tool Steels", <u>8th Congress on Material Testing, Vol.II</u>, Omikk-Technoinform, H-1428 Budapest, Hungary, 1983, pp. 617-21.

19.     Eliasson, L. and Sandberg, O, "Effect of Different Parameters on Heat-Checking Properties of Hot-Work Tool Steels", <u>Neue Werkstoffe und Verfarhen Für Werkzeuge</u>, Berns, H., Nordberg, H. and Fleischer, H.G., eds., Verlag Schrüm und Klagges KG, Bochum, Germany, 1989, pp. 3-14.

20.     Benedyk, J.C., Moracz, D.J. and Wallace, J.F., "Thermal Fatigue Behavior of Die Materials for Aluminum Die Casting", <u>Trans. of the Sixth National Die Casting Congress</u>, SDCE, Detroit MI, 1970, pp. 1-20.

21.     Toyoda, H., Mori, T., Hosomi, K., Hosen, M., Mizuno, Y. and Terabayashi, T., "Thermal Fatigue Properties and Their Evaluation (The Development of Mold Steels With Excellent Thermal Fatigue Properties", <u>Trans ISIJ</u>, 1985, vol. 25, p. B-100.

22.     Ohlson, V., "Development of a Hot-Working Steel for Die Casting, Warm-Pressing and Press Forging", <u>Iron and Steel</u>, August, 1986, pp. 236-238.

23.     Skoff, J.V., "Extended Die Life and Improved Performance Through Comprehensive Stress Texturing", <u>NADCA Transactions</u>, 1989, pp. 1-8.

24.     Centa, L.L. and Wallace, J.F., "Effect of Electro-Discharge Machining on the Surface and Sub-Surface Microstructure of H-13 Steel", <u>NADCA Transactions</u>, 1989, pp. 1-13.

25.     Schindler, A. and Breitler, R., "Die Care Improves Die Life", <u>ADCI Die Tech '84 Technical Seminar</u>, Chicago, IL, 1984, pp. 293-314.

16

26. Rémy, L., Rezai-Aria, F., Danzer, R. and Hoffelner, W., "Evaluation of Life Prediction Methods in High Temperature Fatigue", Low Cycle Fatigue, Solomon, H.D., Halford, G.R., Kaisand I.R. and Leis, B.N., eds., ASTM, Philadelphia, PA, 1988, pp. 1115-1132.

27. Glenny, E. and Taylor, T.A., "A Study of the Thermal-Fatigue Behavior of Metals: The Effect of Test Conditions on Nickel-Base High-Temperature Alloys", Journal of the Institute of Metals, 1959-1960, vol. 88, pp. 449-461.

## DISCLAIMER

Table 1
Nominal Composition of the Standard Grade Wrought and Cast H13 Tool Steel
(All Values in Weight Percent)

| C | Cr | V | Mo | Si | Mn | S | P | Fe |
|---|---|---|---|---|---|---|---|---|
| 0.43 | 5.20 | 0.95 | 1.29 | 1.03 | 0.36 | 0.010 | 0.025 | Balance |

Table 2
Nominal Composition of the Premium Grade Wrought H13 Tool Steel
(All Values in Weight Percent)

| C | Cr | V | Mo | Si | Mn | S | P | Fe |
|---|---|---|---|---|---|---|---|---|
| 0.40 | 5.24 | 0.93 | 1.38 | 1.04 | 0.35 | 0.001 | 0.015 | Balance |

Table 3
Matrix of Heat Checking Experiments
[All Samples Cycled through 1000 (RT→700°C→RT) Cycles]

|  | As-Cast | Cast, Harden and Double Temper | Full Heat Treat | Premium Wrought | Standard Wrought |
|---|---|---|---|---|---|
| 0.5-in. | 2 Samples | 3 Samples | 3 Samples | 3 Samples | 3 Samples |
| 1.5-in. | 5 Samples | 2 Samples | 2 Samples |  |  |

Table 4
ASTM E-45 J-K Inclusion Ratings for H13 Tool Steels

| Condition | Type A (Sulfide-Type) | | Type B (Alumina-Type) | | Type C (Silicate Type) | | Type D (Globular Oxide-Type) | |
|---|---|---|---|---|---|---|---|---|
|  | Thin | Heavy | Thin | Heavy | Thin | Heavy | Thin | Heavy |
| Premium Wrought | 0 | 0 | 0 | 0 | 0 | 0 | 0.5 | 0 |
| Standard Wrought | 1 | 0.5 | 0 | 0 | 0 | 0 | 1 | 0.5 |
| As-Cast (0.5-in) | 0 | 0.5 | 0 | 0 | 0 | 0 | 1 | 1.5 |
| As-Cast (1.5-in) | 0 | 0.5 | 0 | 0 | 0 | 0 | 1 | 1 |
| 0.5-in Partial HT | 0 | 0.5 | 0 | 0 | 0 | 0 | 1 | 1 |
| 0.5-in Full HT | 0.5 | 0 | 0 | 0 | 0 | 0 | 1.5 | 1.5 |
| 1.5-in Partial HT | 0 | 0.5 | 0 | 0 | 0 | 0 | 2 | 1 |
| 1.5-in Full HT | 0 | 0 | 0 | 0 | 0 | 0 | 2 | 1 |
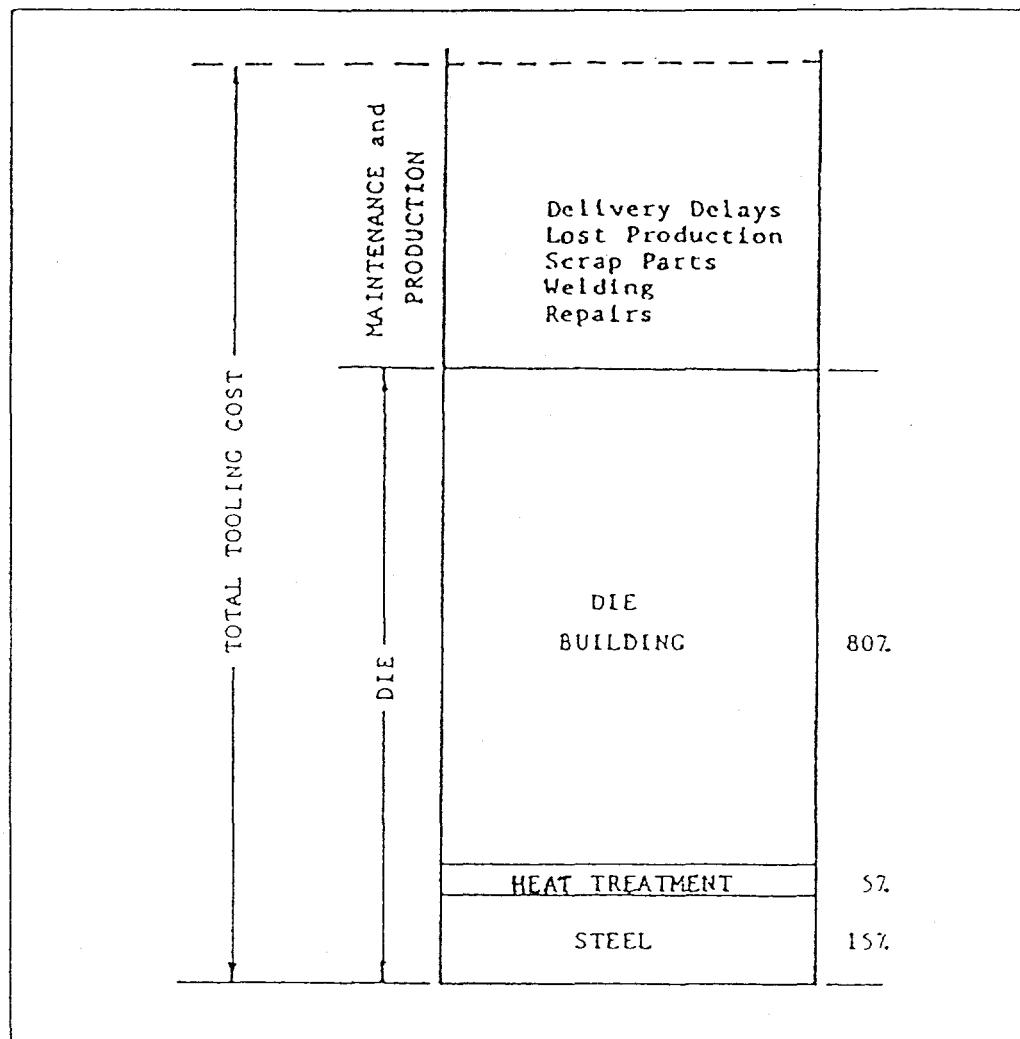
Figure 1.    Schematic diagram showing approximate percentages of costs involved in manufacturing die casting dies (Adapted from Dorsch and Ried[9]).
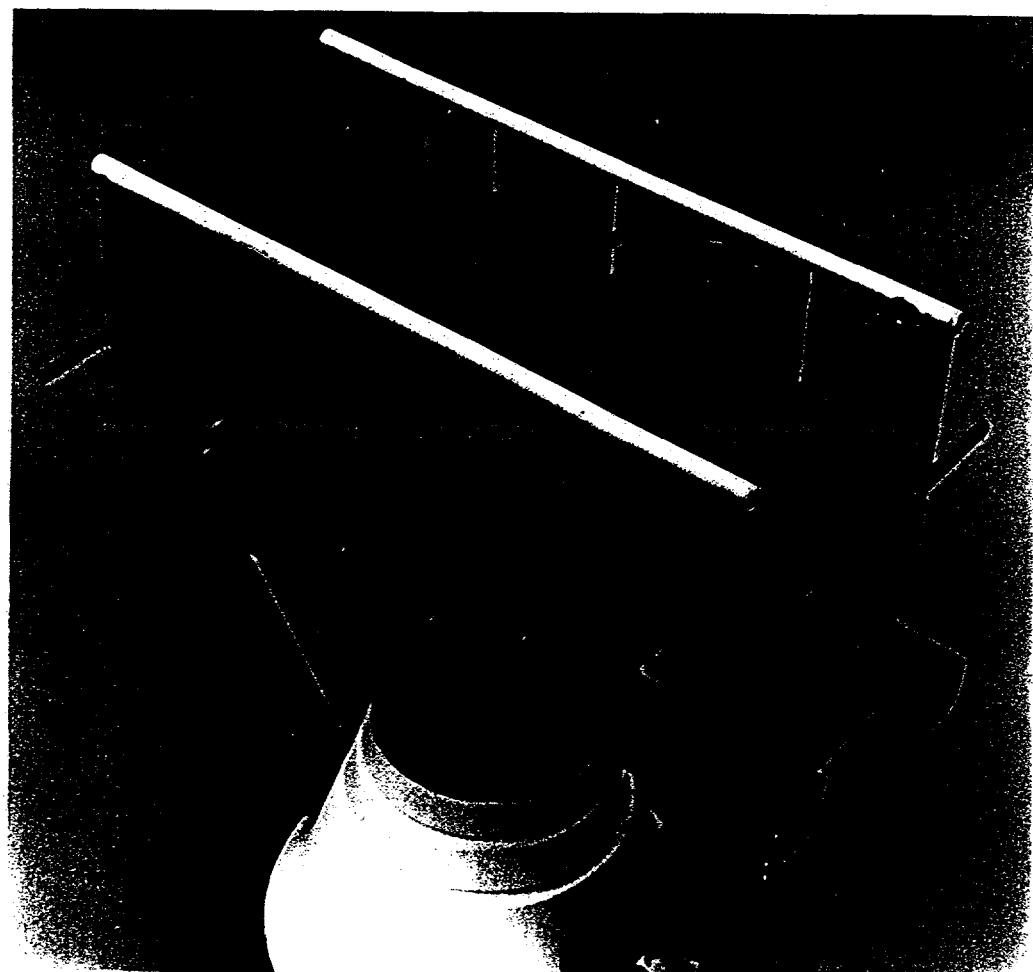
Figure 2.    Wax pattern for the variable microstructure investment castings used to extract samples for heat checking experiments.

Induction Coil

Solenoid Valves

Mac IIx Computer
With NI-MIO-16H Board Installed

Plug to
Auto Switch

On Lepel

Coil Leads
To Lepel

Lexan Box

To Drain
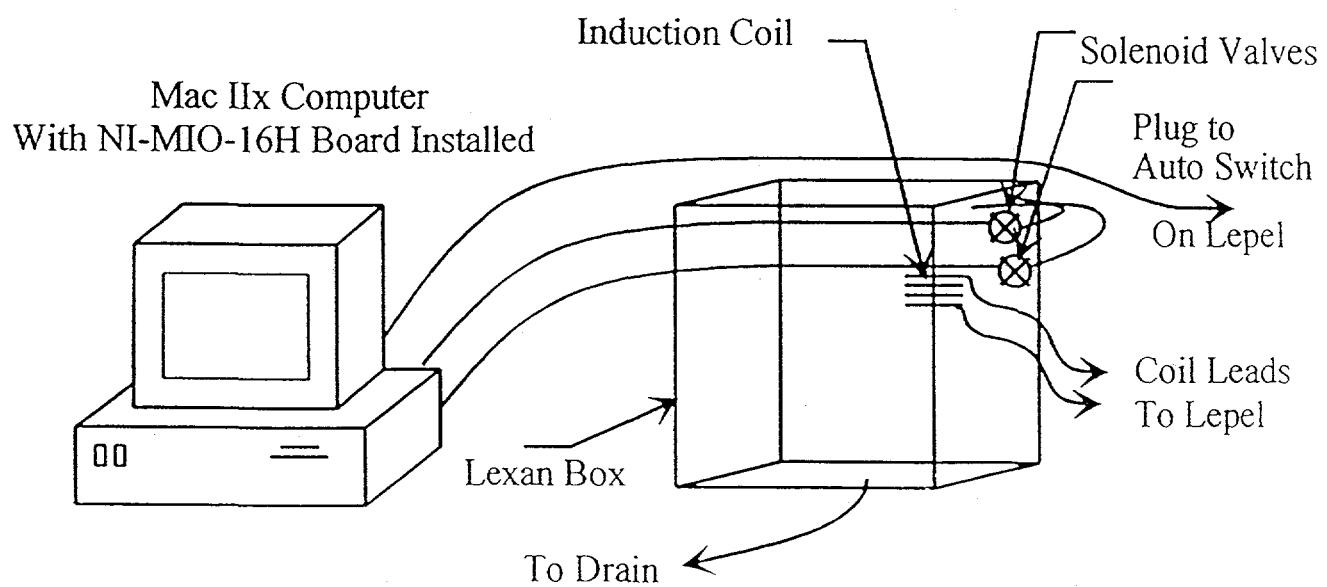
Figure 3.    Schematic design for the thermal fatigue testing unit used at the Colorado
            School of Mines.
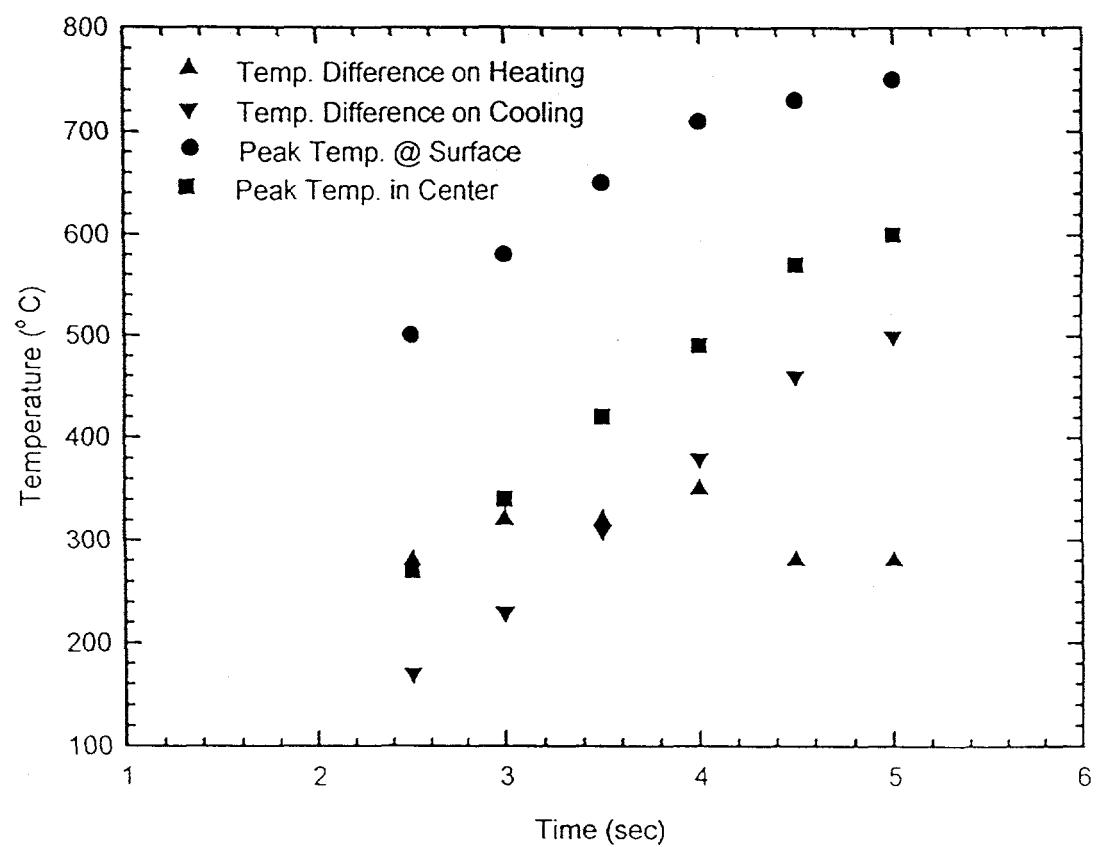
Figure 4.    Calibration curve showing the peak surface and the peak center
temperatures versus generator time on.
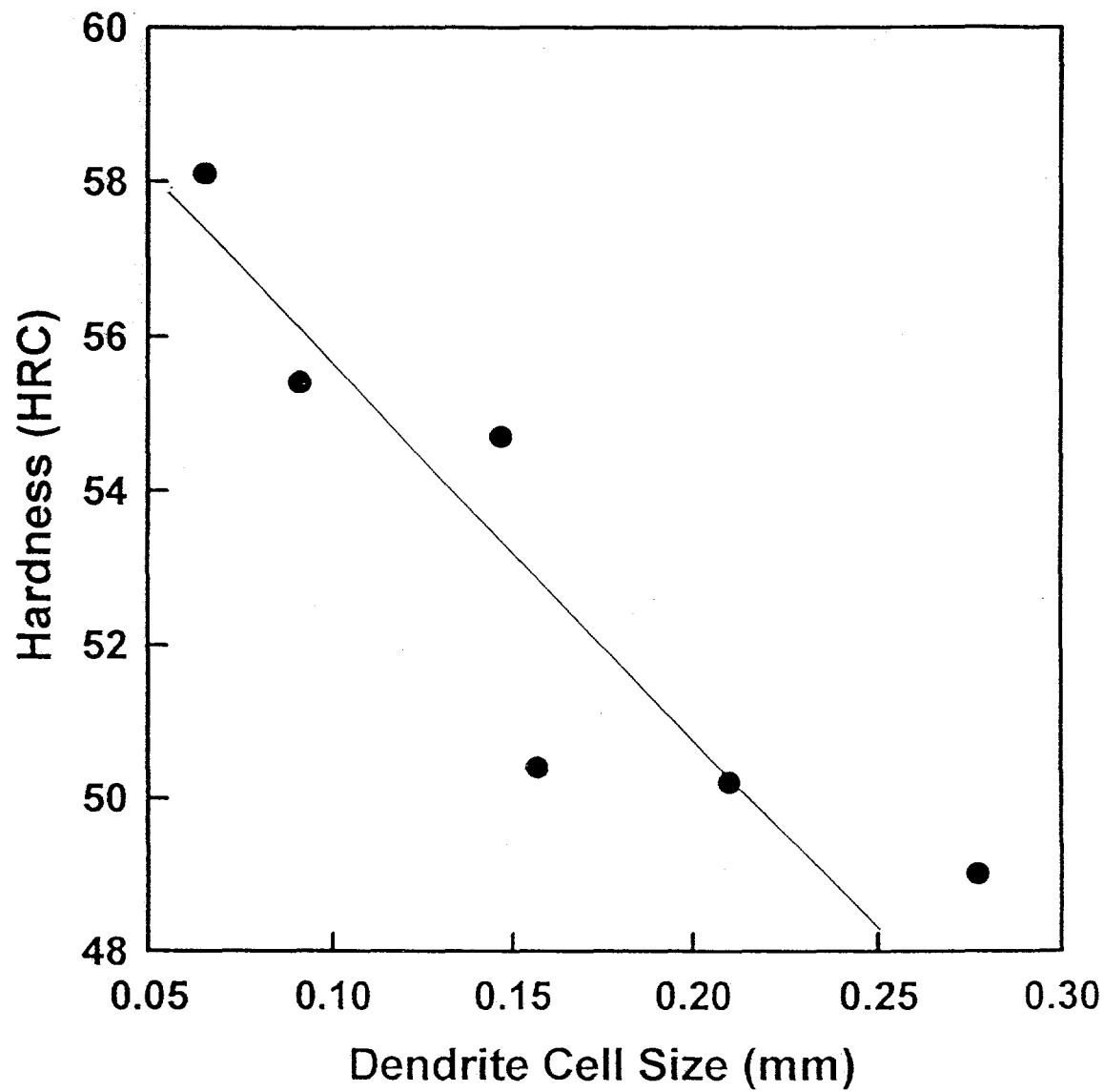
Figure 5.    Hardness of the as-cast samples versus corresponding dendrite cell size for investment cast H13 tool steel.
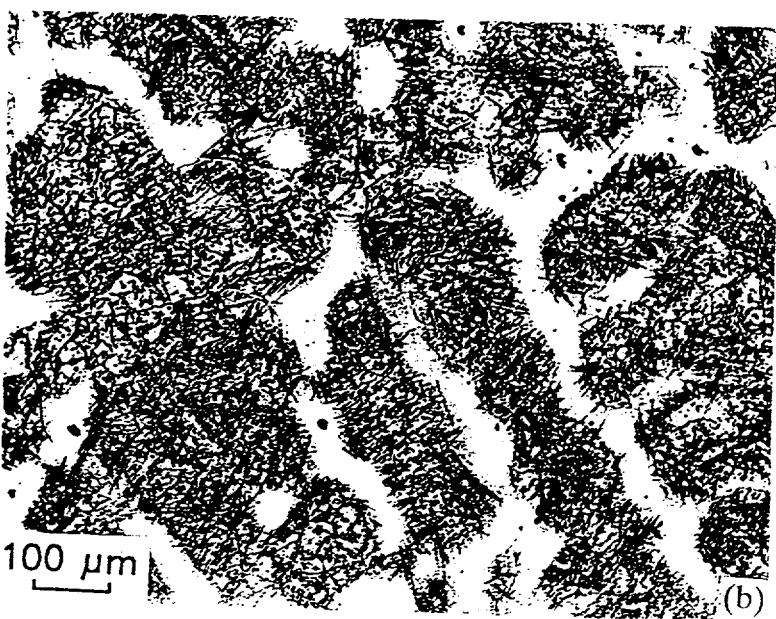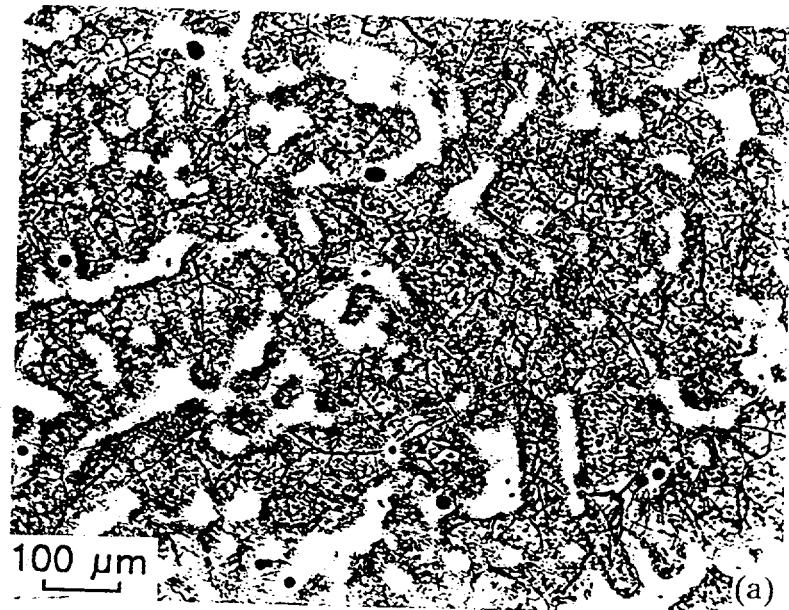
Figure 6.    Light micrographs showing the as-investment cast microstructures of standard grade H13 tool steel; (a) 0.5-in plate and (b) 1.5-in plate.

100 μm (a)

100 μm (b)
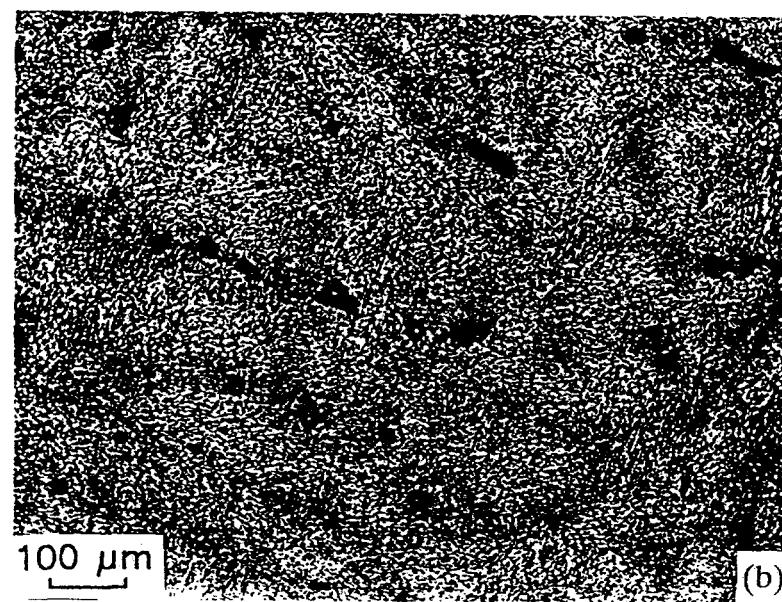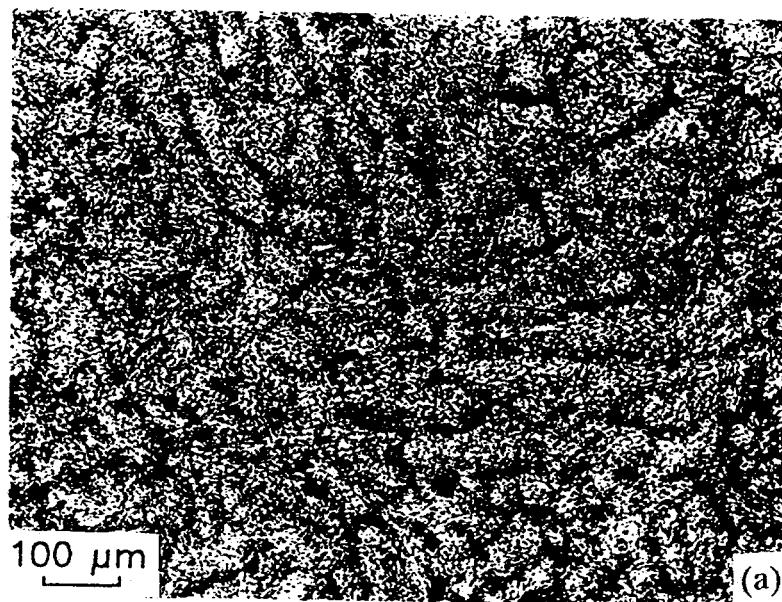
Figure 7.    Light micrographs showing the microstructures resulting from a partial heat treatment of standard grade investment cast H13 tool steel; (a) 0.5-in plate and (b) 1.5-in plate.
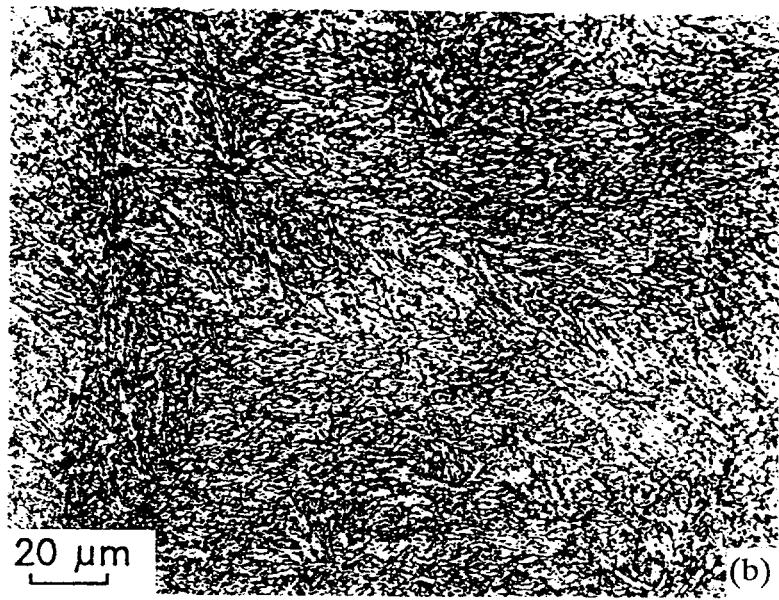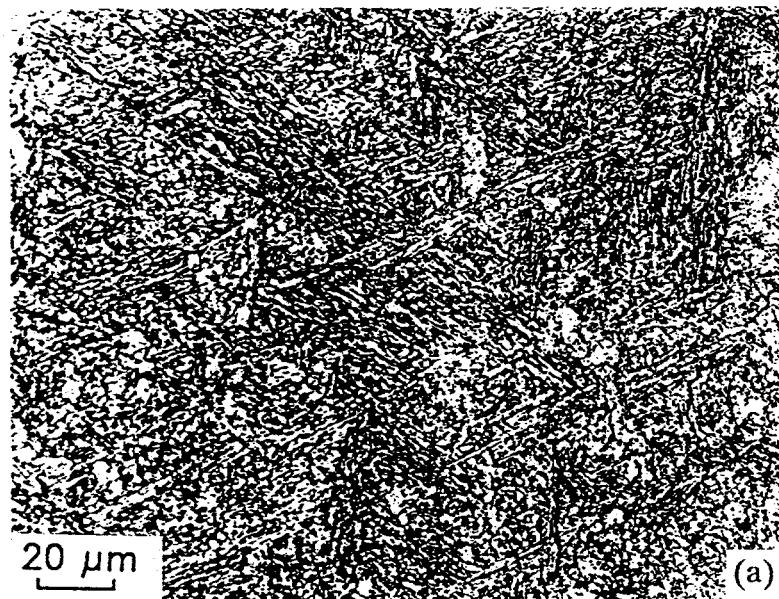
Figure 8.    Light micrographs showing the microstructure resulting from a full heat treatment of standard grade investment cast H13 tool steel; (a) 0.5-in plate and (b) 1.5-in plate.

20 μm
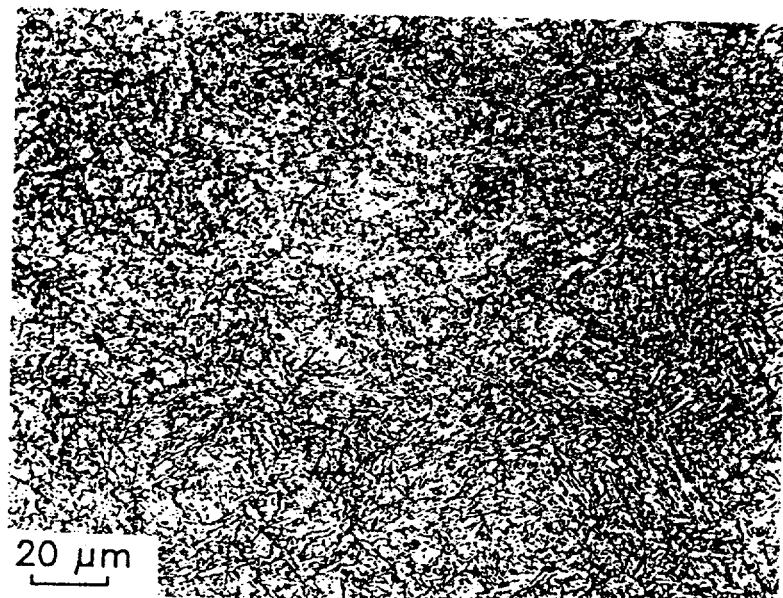
Figure 9.    Light micrograph showing the microstructure of standard grade wrought
H13 tool steel after the double temper treatment.
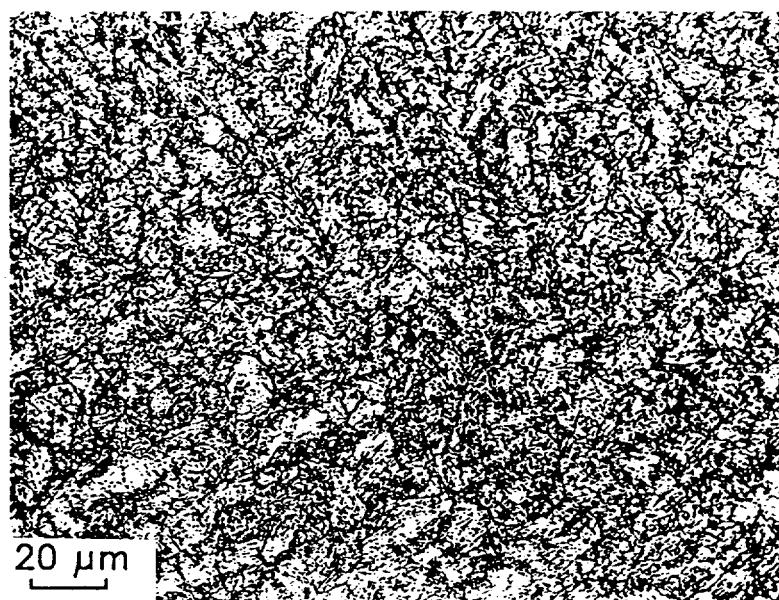
Figure 10.    Light micrograph showing the microstructure of premium grade wrought
             H13 tool steel after the double temper treatment.
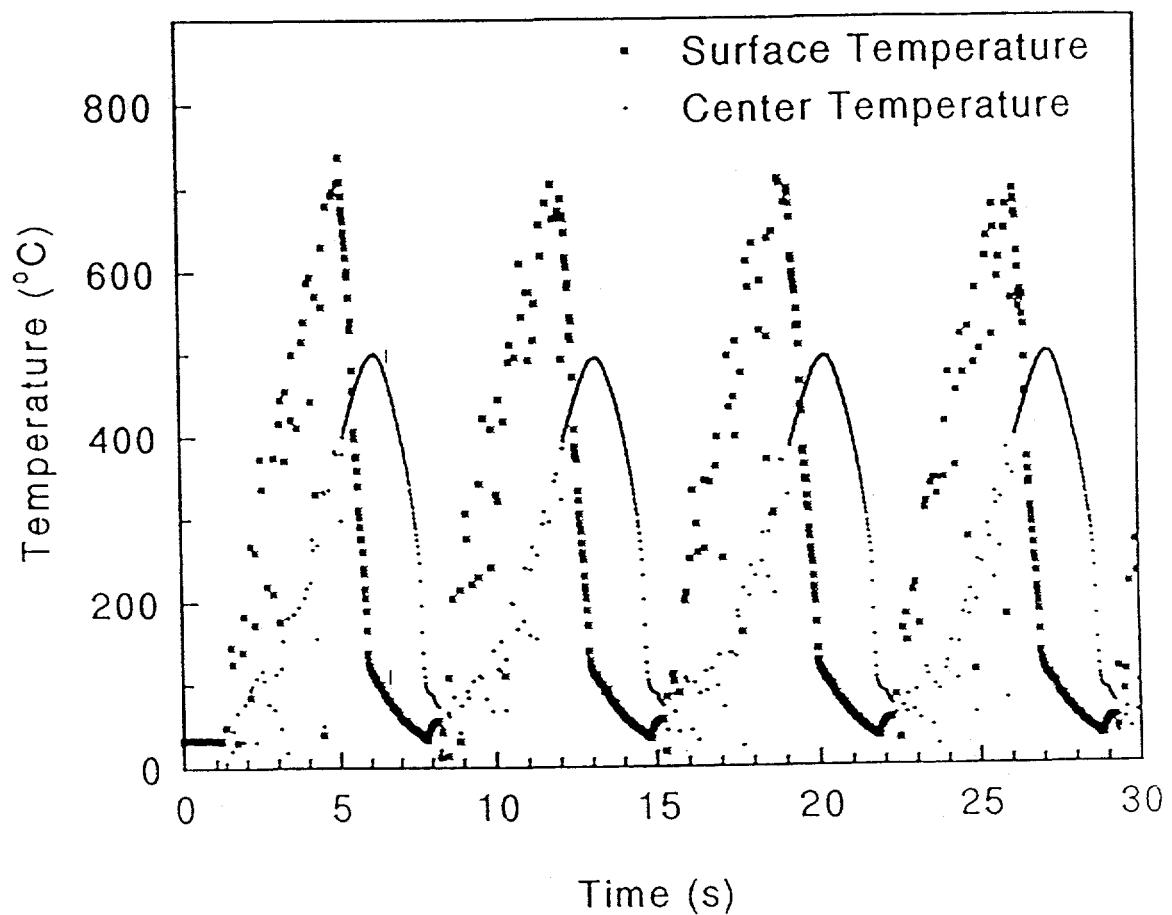
Figure 11. Time-temperature profile of the RT → 1295°F (700°C) → RT cycles used in the thermal fatigue tests. The cycle incorporated a 4 second heating time, a 2 second water-quench, and a 1 second air-blast in each cycle.
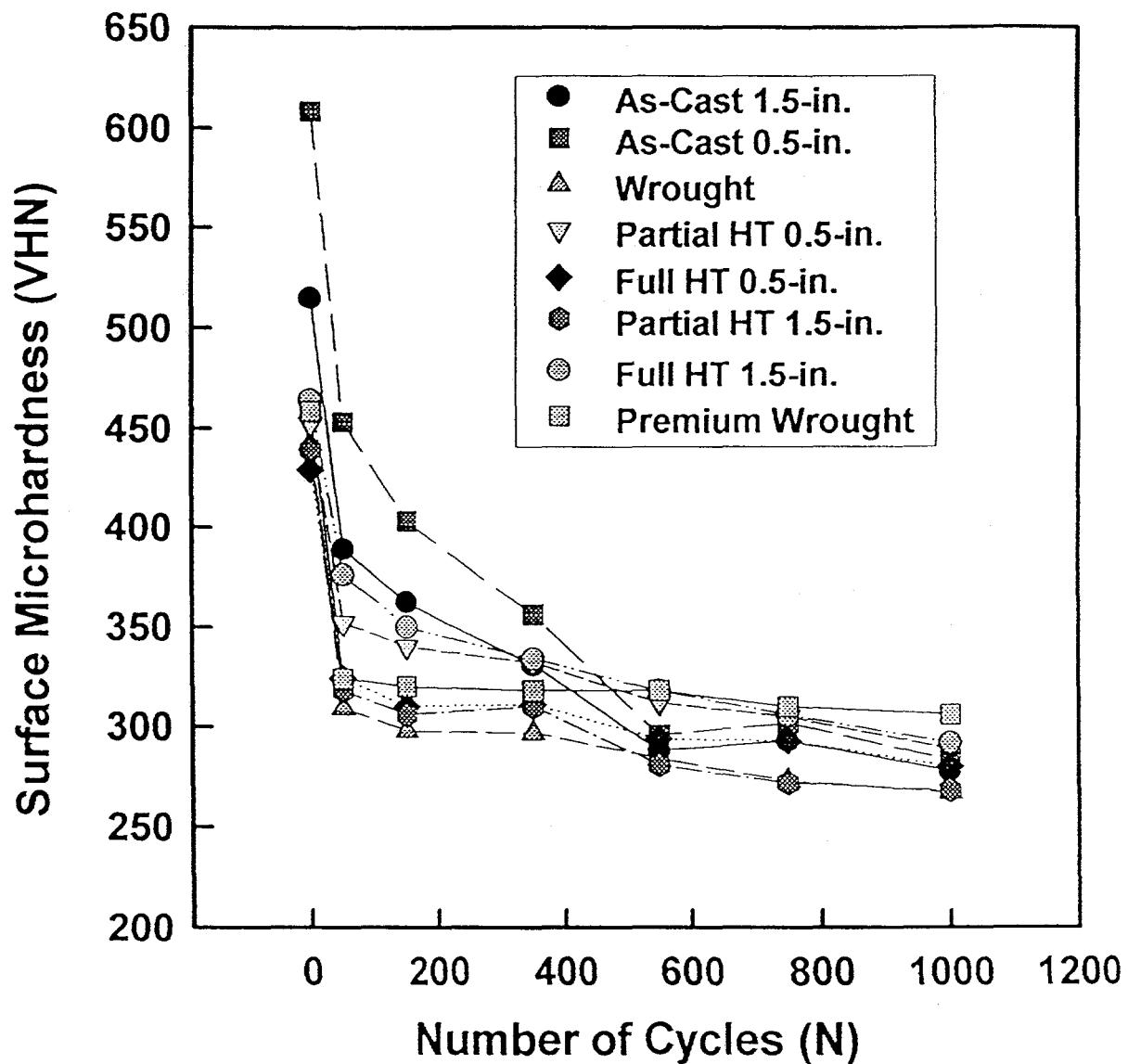
Figure 12.    Summary plot of surface microhardness versus the number of thermal cycles.
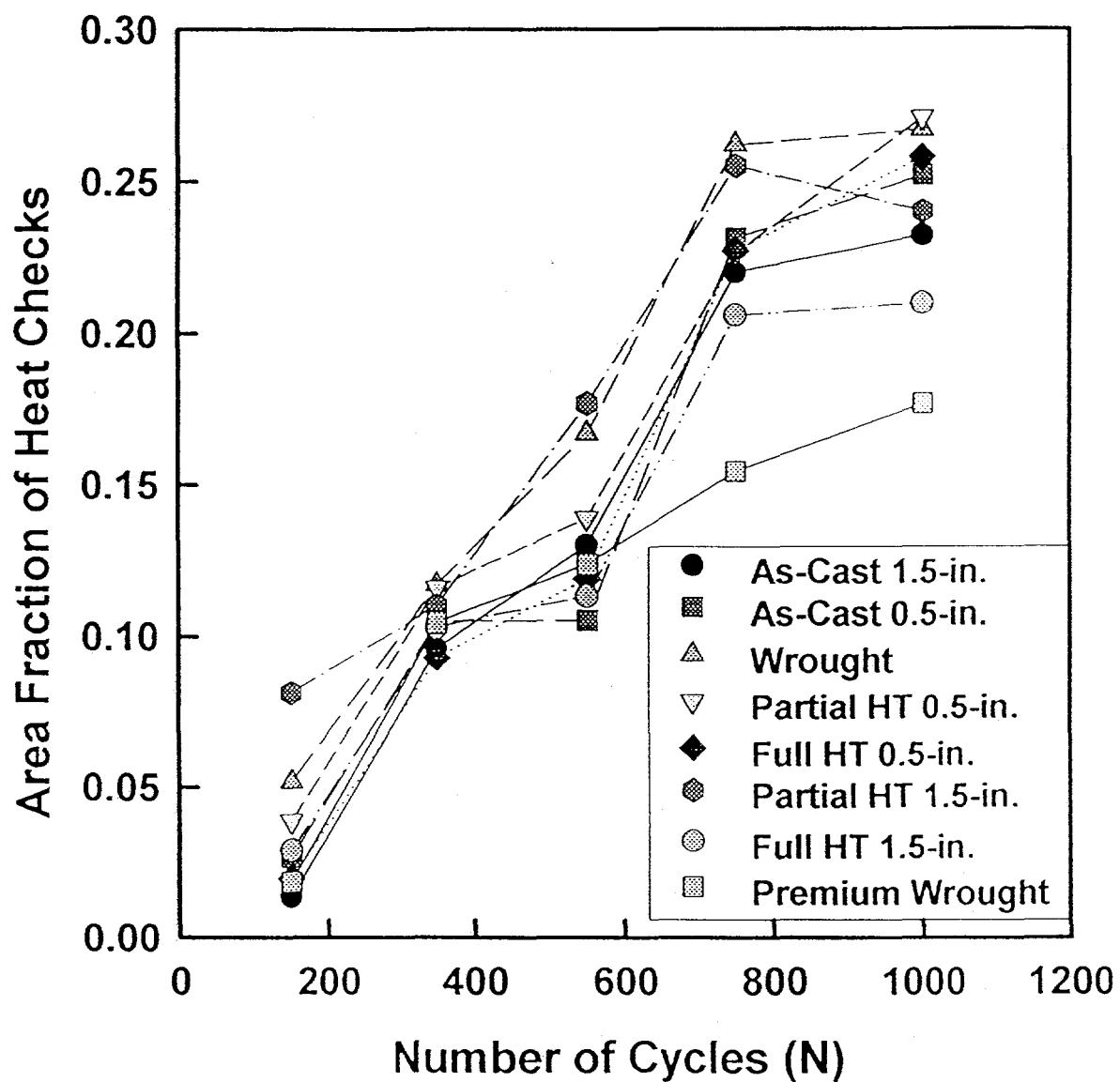
Figure 13.    Summary plot of area fraction of heat checks versus the number of thermal cycles.
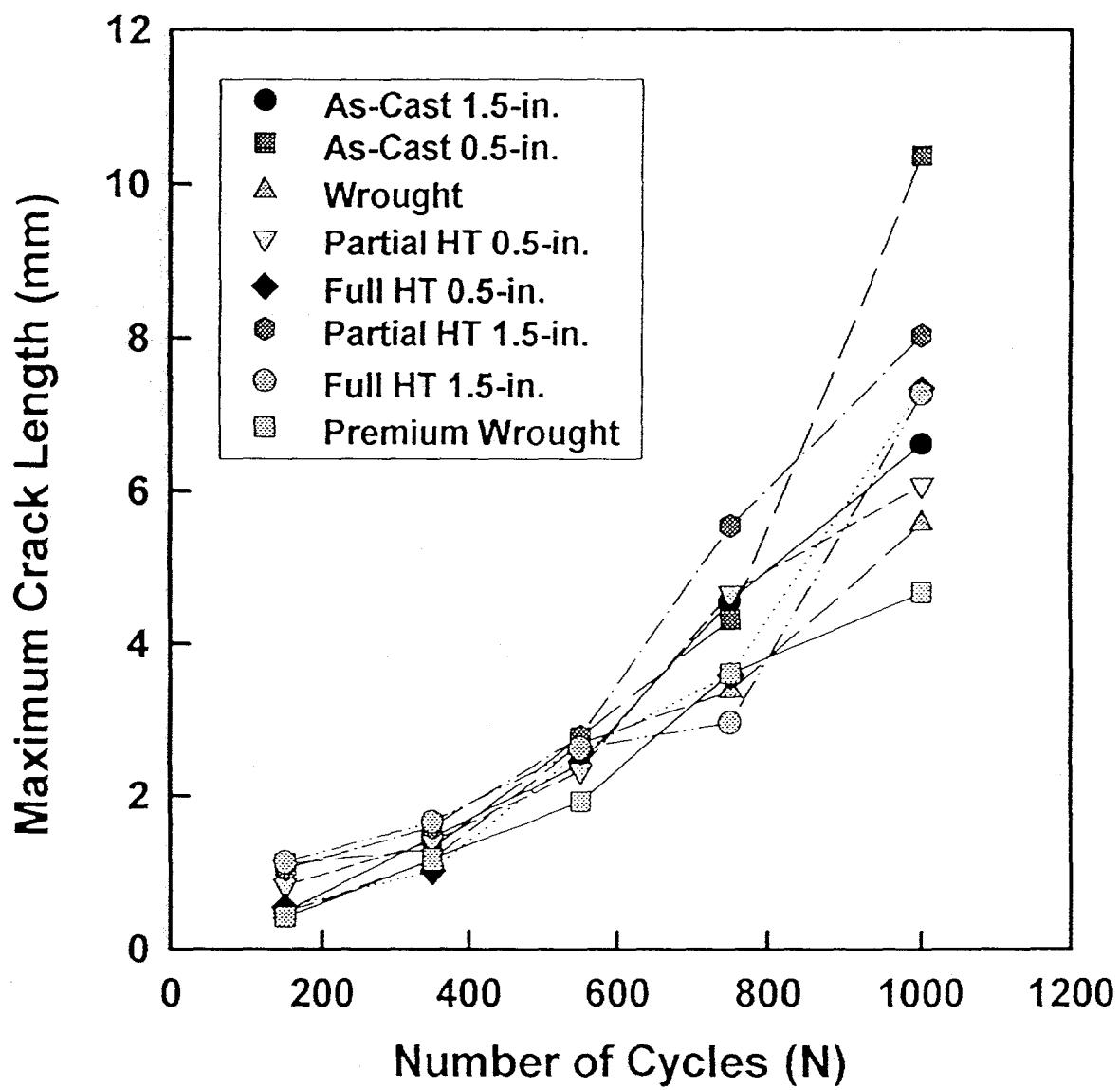
Figure 14.    Summary plot of maximum crack length on the sample surface versus the
number of thermal cycles.

**As-Cast 1.5-in Plate (700°C Cycles)**

95% Confidence

*Y-axis: Area Fraction of Heat Checks (0.00 – 0.30)*

*X-axis: Number of Cycles (N) (0 – 1200)*
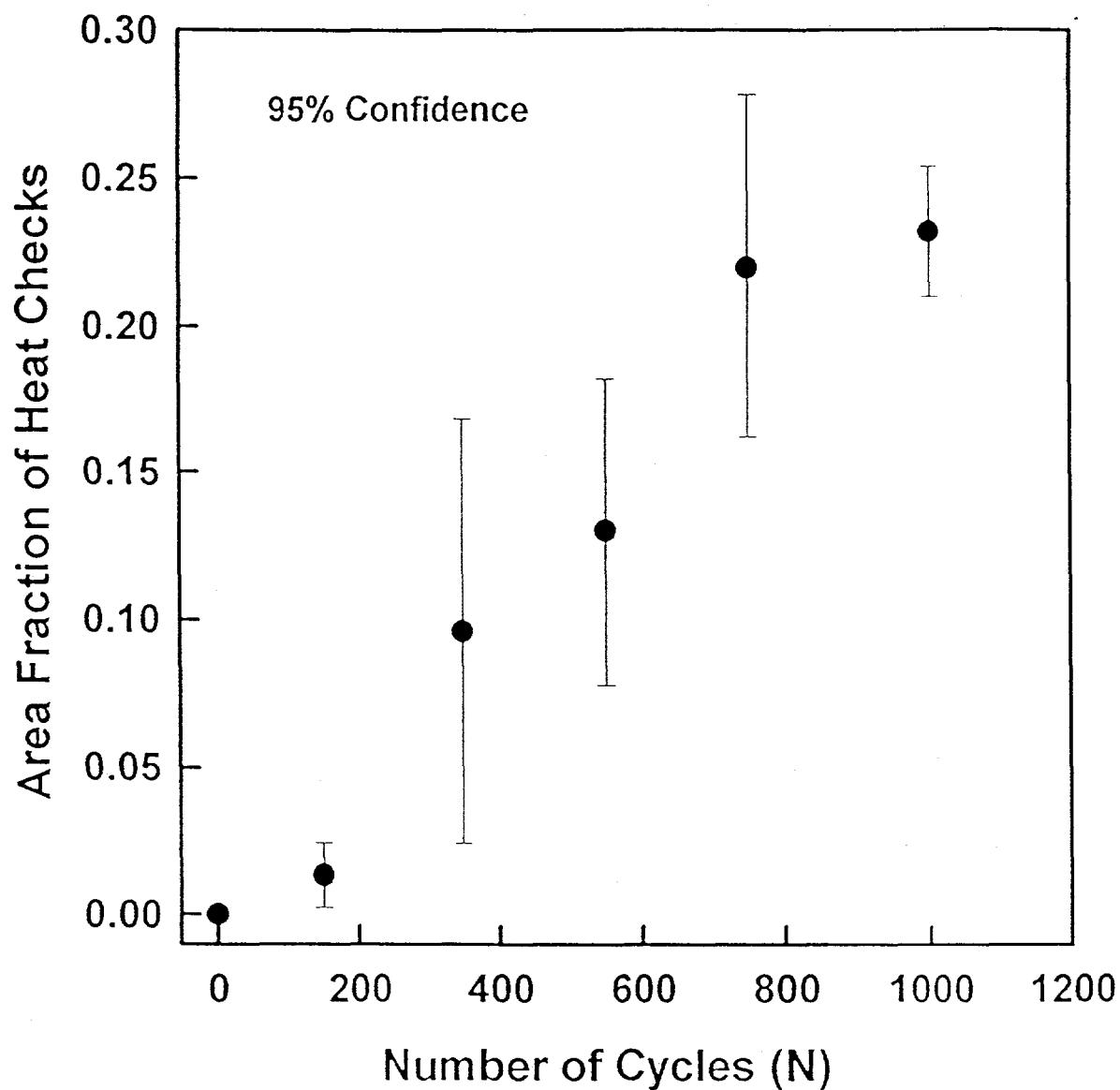
Figure 15.    Plot of area fraction of heat checks versus the number of thermal cycles for as-cast 1.5-in plate H13 tool steel. Error bars were placed at 95% confidence.

## After 1000 700°C Cycles
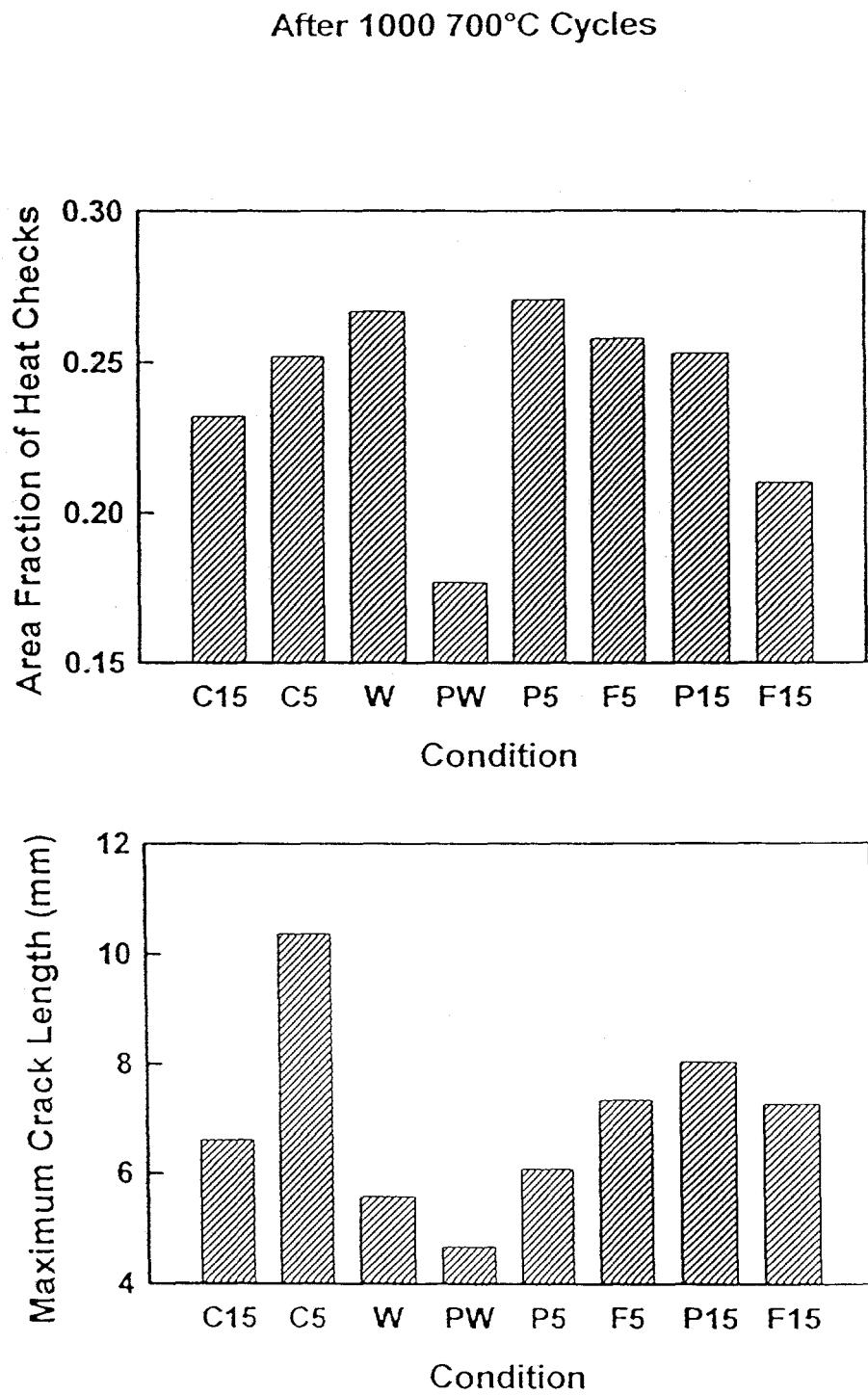


Figure 16. Summary plot of area fraction of heat checks and maximum crack length after 1000 thermal cycles versus the sample condition.
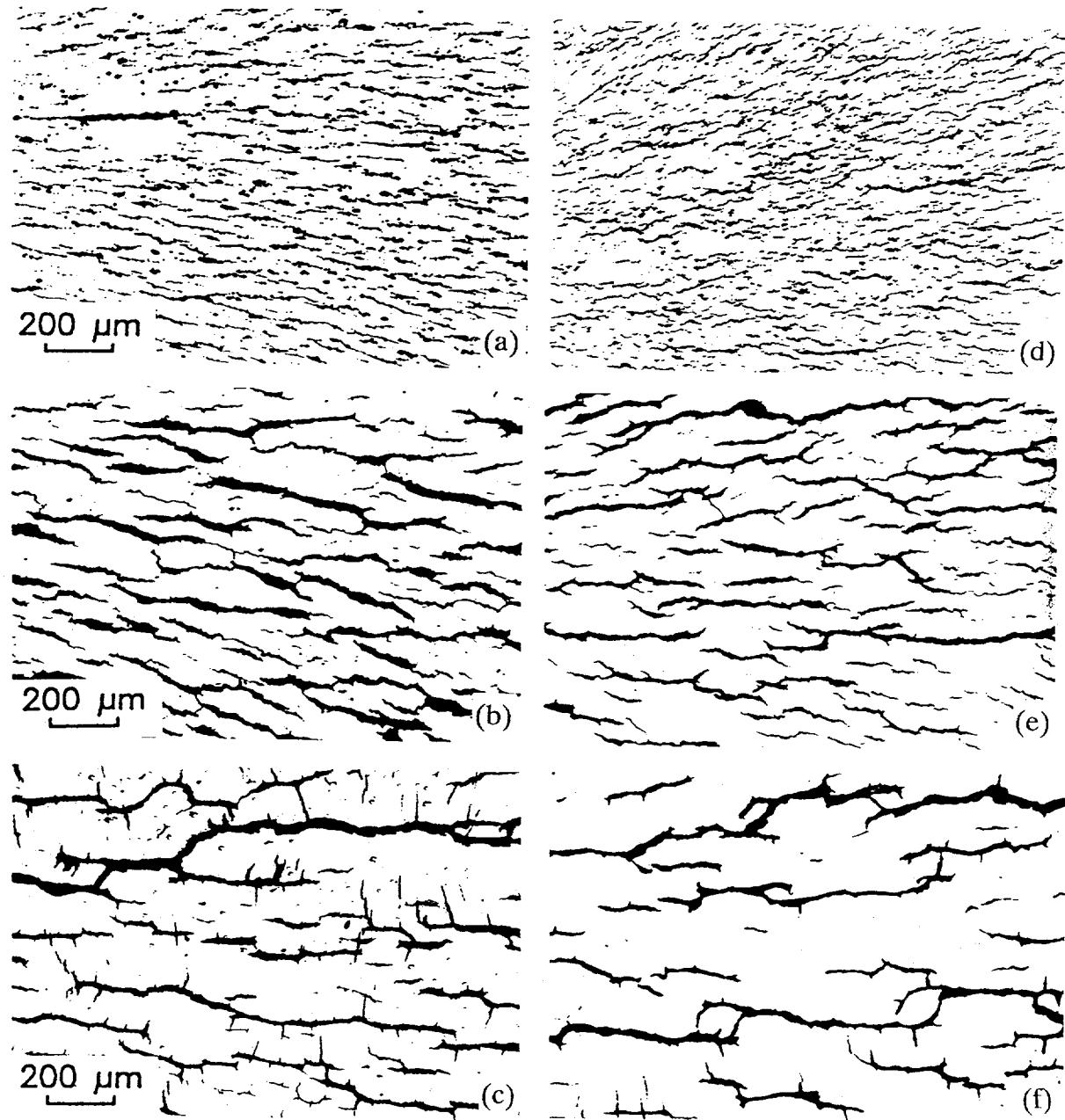
Figure 17.    Micrographs showing heat checking on the surfaces of standard grade and premium grade wrought H13 tool steel (a) standard wrought material after 150 cycles, (b) standard wrought material after 550 cycles, (c) standard wrought material after 1000 cycles, (d) premium wrought material after 150 cycles, (e) premium wrought material after 550 cycles and (f) premium wrought material after 1000 cycles.
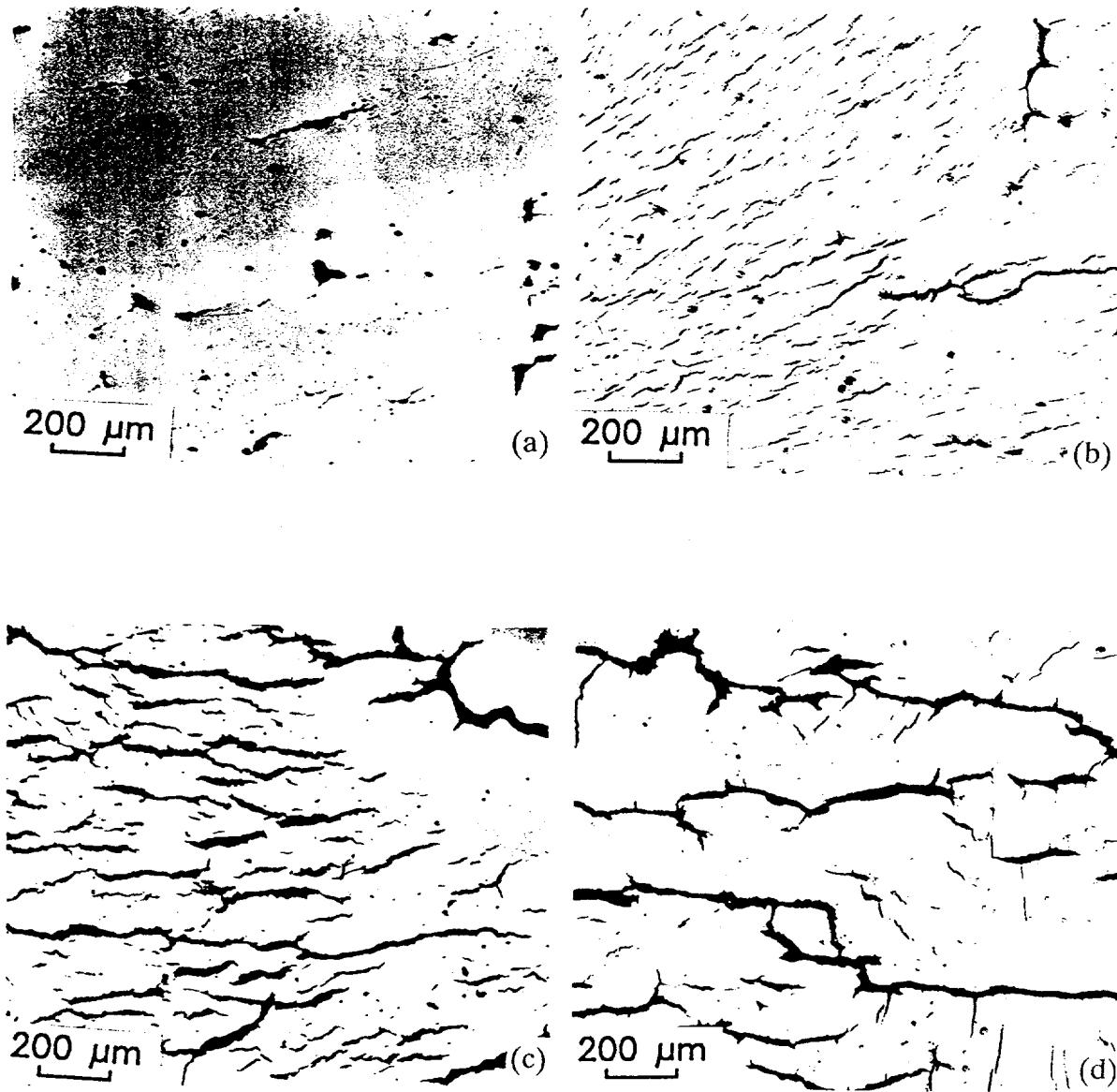
Figure 18.     Micrographs showing heat checking on the surface of as-cast 1.5-in plate
H13 tool steel; (a) after 50 thermal cycles, (b) after 150 thermal cycles, (c)
after 550 thermal cycles, and (d) after 1000 thermal cycles.
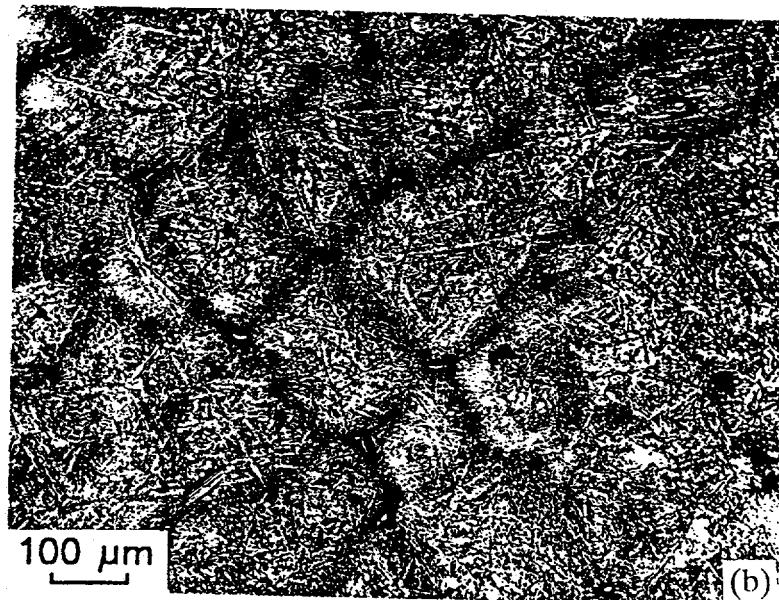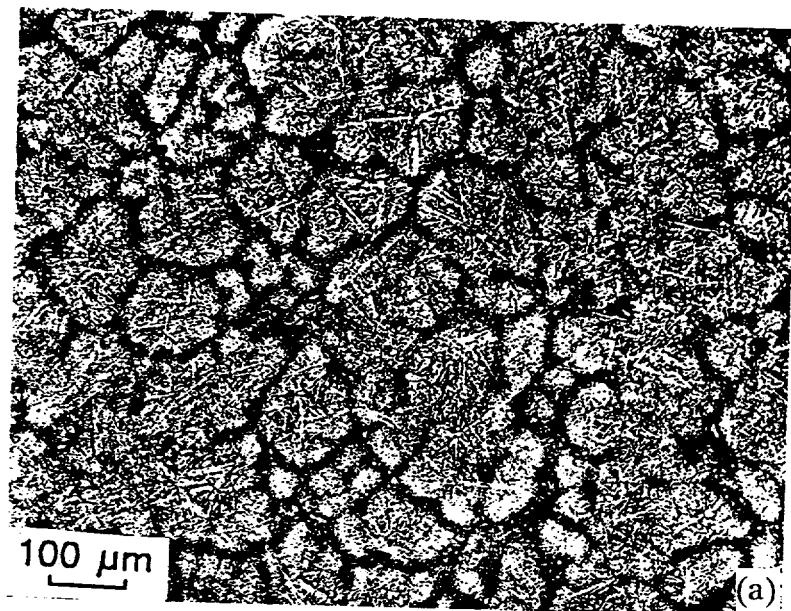
Figure 19.    Micrographs depicting the microstructures of as-cast material after 1000 thermal cycles: (a) as-cast 0.5-in plate material and (b) as-cast 1.5-in plate material.
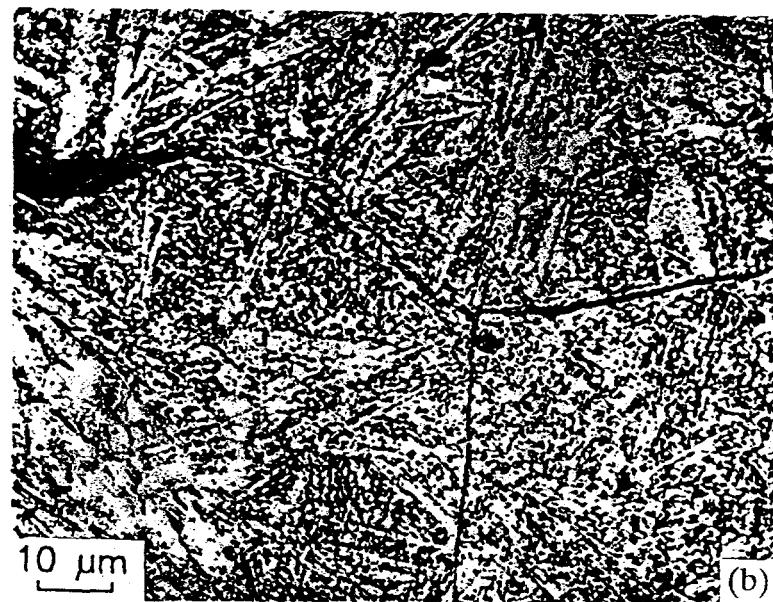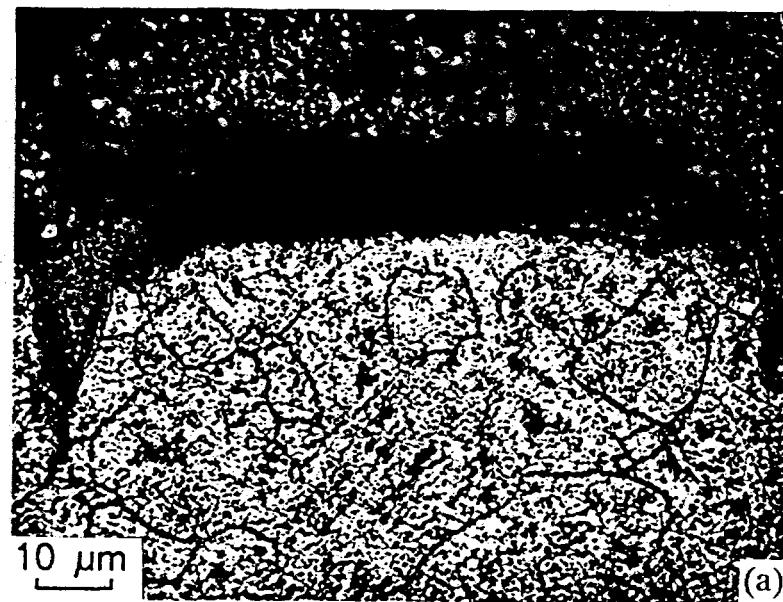
Figure 20.    Microstructural evidence for intergranular oxidation cracking in H13 tool
steel: (a) premium grade wrought H13 tool steel after 1000 cycles and (b)
as-cast 1.5-in plate H13 tool steel after 1000 cycles.
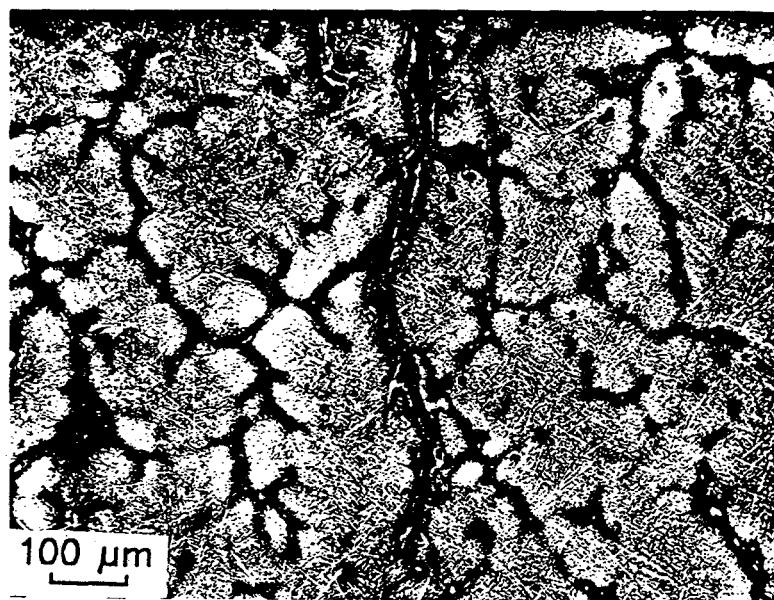
Figure 21.    Microstructural evidence for interdendritic cracking in as-cast 0.5-in plate
H13 tool steel.